Molecular Catalysis 475 (2019) 110403

Contents lists available at ScienceDirect

Molecular Catalysis

journal homepage: www.elsevier.com/locate/mcat

Synthesis of pyridinium-based salts: Catalytic application at the synthesis of six membered *O*-heterocycles

Saeed Babaee[a], Mohammad Ali Zolfigol[a,*], Mahmoud Zarei[a,*], Maryam Abbasi[a], Zahra Najafi[b]

[a] Department of Organic Chemistry, Faculty of Chemistry, Bu-Ali Sina University, Hamedan 6517838683, Iran
[b] Department of Medicinal Chemistry, School of Pharmacy, Hamadan University of Medical Sciences, Hamadan, Iran

ARTICLE INFO

Keywords:
2-Amino-4*H*-chromene
2-Amino-4,8-dihydropyrano
2-Amino-4H-pyrans
Anion exchange
Drug candidates
Magnetic molten salts
Molten salts
O-heterocyclic compounds
$[PySO_3H]FeCl_4$
$[PySO_3H]AlCl_4$
$[PySO_3H]BF_4$
$[PySO_3H]PF_6$

ABSTRACT

In this paper, a range of pyridinium-based ionic liquid (IL) and molten salts (MSs) with various counter ions were designed, synthesized and fully characterized. These novel ionic liquid and molten salts were prepared via the reaction of $[PySO_3H]Cl$ with $AlCl_3$, $FeCl_3$, $NaBF_4$ and KPF_6 to produce the desired catalysts $[PySO_3H]X$ (X = $AlCl_4$, $FeCl_4$, BF_4 and PF_6). The structure of these catalysts were investigated by FT-IR, NMR (^1H, ^{13}C, ^{27}Al, ^{19}F) and mass spectra as well as the use of the XRD, SEM, TG, DTG and DTA techniques. Magnetic measurements (VSM) of $[PySO_3H]FeCl_4$ as a magnetic molten salts was also investigated. Three categories of six membered *O*-heterocyclic compounds such as 2-amino-4*H*-chromene, 2-amino-4,8-dihydropyrano and 2-amino-4*H*-pyrans were prepared in the presence of a catalytic amount of the above said molten salts. These synthesized *O*-heterocyclic compounds are highly regarded due to their biological activities.

Introduction

Anion exchange is a subjective way for designing and synthesis of ionic liquids (ILs) or molten salts (MSs) with a wide range of counter ions which cannot be directly prepared. Nowadays, the physico-chemical properties of ILs and MSs such as: viscosity, melting point, vapor pressure of fluids and fluorescence had been changed via the exchanging of their counter ions [1–4]. By changing physical and chemical properties of ILs and MSs, their catalytic ability will be also change. Ionic liquids and molten salts as efficient catalysts and/or reagents were applied for nitration reaction, regioselective sulfonation, preparation of energetic compounds and other organic synthesis under milder conditions [5–10].

A variety of compounds have been used for the synthesis of ionic liquids, which have revealed various catalytic and chemical properties. Ionic liquids as dual role catalysts with both Brønsted and Lewis acidic properties have high catalytic abilities [2,5,11–20]. Due to the design ability of ionic liquids, these catalysts in perennials have been used for the synthesis of a various kinds of biological and pharmaceutical candidate compounds [21].

The presence of oxygen atoms in the structure of the heterocyclic compounds leads to the creation of biological properties of *O*-heterocyclic structures [22,23]. Cyclic structures with oxygen rings have been observed in the structures of various pharmaceutical compounds such as anti-cancer [24], anti-alzheimer [25], anti-malarial [26] and other biological active compounds [25]. The presence of 2-amino-4*H*-chromene, 2-amino-4,8-dihydropyrano and 2-amino-4*H*-pyrans rings in the molecular structures, naturally produces a spectrum of biological properties such as antitumor [27], antioxidants [28] and antifungal [29]. The presence of these biological properties is the major reason for the developing of various methodologies at the synthesis of described valuable compounds [30–36].

Due to the above facts and on the basis of our previous investigations on the field of ILs and MSs with chlorosulfonic acid [37,38], we were interested on the development of anion exchange method for the synthesis of ionic liquid {$[PySO_3H]BF_4$, m.p. 85–88 (°C)}, molten salts {$[PySO_3H]AlCl_4$, m.p. > 300 (°C)}, {$[PySO_3H]PF_6$, m.p. 258–260 (°C)} and {$[PySO_3H]FeCl_4$, m.p. 266 dec}. The ionic liquid (IL) $[PySO_3H]BF_4$ and above said molten salts (MSs) $[PySO_3H]X$ (X = $FeCl_4$, $AlCl_4$ and BF_4) were utilized as efficient and reusable catalysts for the preparation of a wide range of *O*-heterocyclic compound (2-amino-4*H*-chromene, 2-amino-4,8-dihydropyrano and 2-amino-4H-pyrans) through the condensation reaction of aldehyde, malononitrile and 2-hydroxynaphtalen-1,4-dione, 5-Hydroxy-2-(hydroxymethyl)-4*H*-pyran-4-one or Ethyl

* Corresponding authors.
E-mail addresses: zolfi@basu.ac.ir, mzolfigol@yahoo.com (M.A. Zolfigol), mahmoud8103@yahoo.com (M. Zarei).

https://doi.org/10.1016/j.mcat.2019.110403
Received 24 January 2019; Received in revised form 9 May 2019; Accepted 11 May 2019
2468-8231/ © 2019 Published by Elsevier B.V.

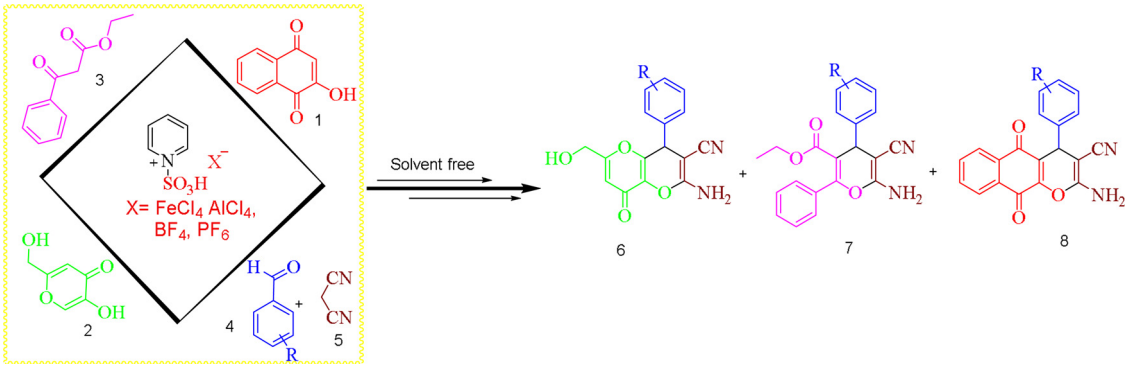

Scheme 1. Synthesis of *O*-heterocyclic compounds using $[PySO_3H]X$ (X = $FeCl_4$ BF_4, PF_6 or $AlCl_4$).

benzoyl acetate under mild, green and solvent-free conditions (Scheme 1).

Experimental

General procedure for the preparation of molten salts $[PySO_3H]X$ (X = $FeCl_4$, BF_4, PF_6 or $AlCl_4$)

At first, ionic liquid $[PySO_3H]Cl$ was synthesized according to our previously reported procedure [39]. A mixture of $[PySO_3H]Cl$ (5 mmol, 0.975 g) and one of the inorganic salts ($AlCl_3$, $FeCl_3$, $NaBF_4$ or KPF_6) (5 mmol) was placed into a mortar and warmed up to at 60 °C, and the reaction mixture grinded by a pestle for two hours. After completion of the reaction, the reaction mixture was cool down to room temperature, ethanol was used to purify the obtained ILs and MSs. molten salts $[PySO_3H]FeCl_4$, $[PySO_3H]PF_6$, $[PySO_3H]AlCl_4$ and ionic liquid $[PySO_3H]BF_4$ were obtained in (1.76 g) 99%, (1.46 g) 96%, (1.61 g) 99% and (1.17 g) 95%, yields, respectively (Scheme 2).

General procedure for the synthesis of O-heterocyclic compounds (2-amino-4H-chromene, 2-amino-4,8-dihydropyrano and 2-amino-4H-pyrans)

The mixture of *O*-derivatives (2-hydroxynaphtalen-1,4-dione, 5-hydroxy-2-(hydroxymethyl)-4*H*-pyran-4-one or ethyl benzoylacetate) (1 mmol), malononitrile (1 mmol, 0.066 g) and aldehyde (1 mmol) in the presence of 10 mol% of molten salts $[PySO_3H]PF_6$ (0.03 g), $[PySO_3H]AlCl_4$ (0.033 g), $[PySO_3H]FeCl_4$ (0.035 g) or 15 mol% ionic liquid $[PySO_3H]BF_4$ (0.037 g) in a 25 ml round-bottomed flask was stirred at 90 °C under solvent-free condition. After the completion of the reactions which were monitored by the TLC technique (4/6 *n*-hexane: ethyl acetate). Then, 10 ml of acetone was added to the reaction mixture and the described catalysts (which are not soluble in the acetone) were subsequently removed by centrifugation (1000 rpm). Finally, after the evaporation of the solvent at room temperature, the product was purified with ethyl acetate (Scheme 1).

2. -Amino-5,10-dioxo-4-(p-tolyl)-5,10-dihydro-4*H*-benzo[*g*]chromene-3-carbonitrile (6b)

Orange solid; Mp: 263–265 °C; IR (KBr): υ (cm^{-1}) = 3400, 3334, 3207, 2962, 2197, 1692, 1670; ^{1}H NMR (300 MHz, DMSO-d_6) δ $_{ppm}$: 8.12 - 7.99 (m, 1 H), 7.86 (dtd, *J* = 8.6, 5.3, 2.0 Hz, 3 H), 7.31 (s, 2 H), 7.19 (d, *J* = 7.8 Hz, 2 H), 7.11 (d, *J* = 7.9 Hz, 2 H), 4.57 (s, 1 H), 2.25 (s, 3 H). ^{13}C NMR (75 MHz, DMSO-d_6) δ $_{ppm}$: 183.0, 177.3, 158.8, 149.2, 141.1, 136.7, 135.0, 134.6, 131.5, 131.1, 129.6, 128.0, 126.5, 126.2, 122.6, 58.1, 36.6, 21.2.

2. -Amino-4-(3,5-difluorophenyl)-5,10-dioxo-5,10-dihydro-4*H*-benzo[*g*]chromene-3-carbonitrile (6i)

Orange solid; Mp: 260–263 °C; IR (KBr): υ (cm^{-1}) = 3396, 3316, 3193, 2199, 1622, 1667, 1622; ^{1}H NMR (400 MHz, DMSO-d_6) δ $_{ppm}$: 8.09–8.05 (m, 1 H), 7.93–7.80 (m, 4 H), 7.43 (s, 1 H), 7.18–7.11 (m, 3 H), 7.11–7.06 (m, 1 H), 4.71 (s, 1 H). ^{13}C NMR (101 MHz, DMSO-d_6) δ $_{ppm}$: 182.5, 176.7, 163.6, 163.5, 161.2, 161.1, 158.2, 158.2, 149.6, 148.3, 148.2, 148.1, 134.4, 134.1, 130.9, 130.8, 156.0, 125.8, 120.1, 119.0, 119.0, 111.1, 111.0, 110.9, 110.8, 102.8, 102.5, 102.3, 56.6, 36.2.

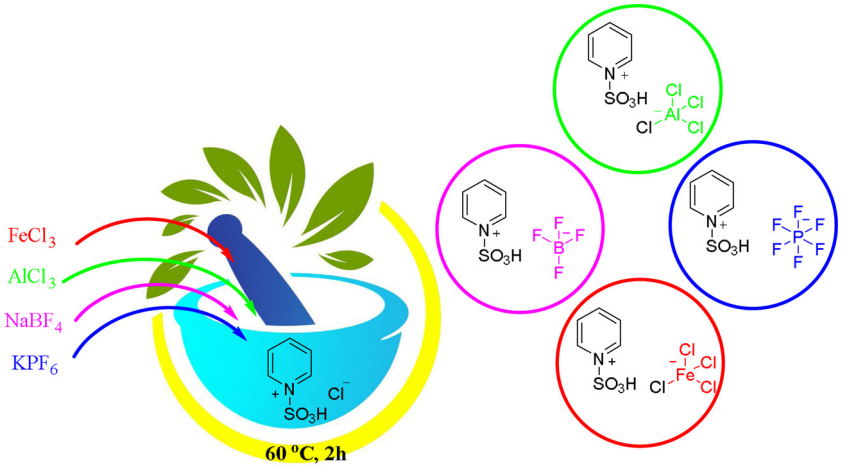

Scheme 2. Synthesis of ionic liquid and molten salts $[PySO_3H]X$ (X = $FeCl_4$, BF_4, PF_6 or $AlCl_4$).

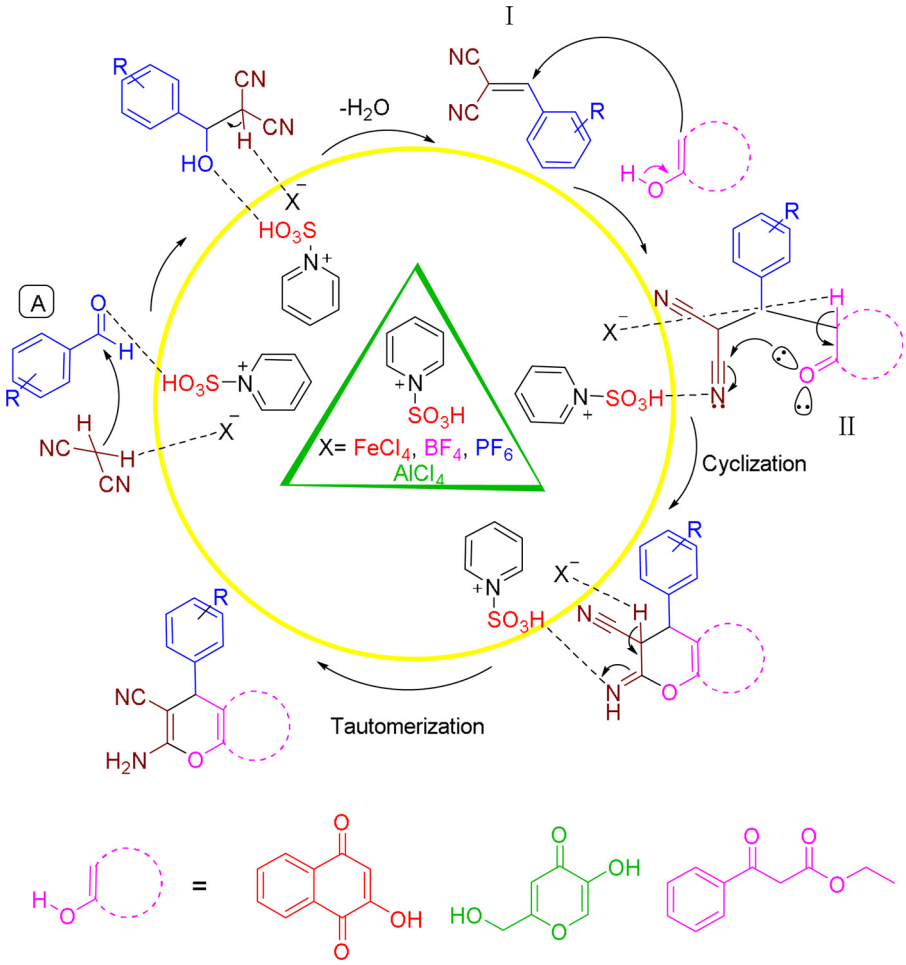

Scheme 3. Proposed mechanism for the synthesis *O*-heterocycle compounds using [$PySO_3H$]X (X = $FeCl_4$, $AlCl_4$, BF_4 and PF_6).

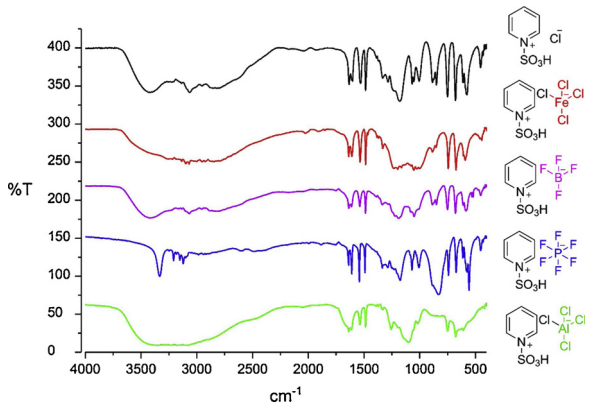

Fig. 1. FT-IR of [$PySO_3H$]X (X = $FeCl_4$, BF_4, PF_6 or $AlCl_4$) and [$PySO_3H$]Cl in KBr.

2. -Amino-6-(hydroxymethyl)-4-(4-nitrophenyl)-8-oxo-4,8-dihydropyrano[3,2-*b*] pyran-3-carbonitrile (7e)

White solid; Mp: > 300 °C; IR (KBr): υ (cm^{-1}) = 3537, 3454, 3328, 3176, 2923, 2195, 1673, 1650, 1520, 1350; ^{1}H NMR (400 MHz, DMSO-d_6) δ $_{ppm}$: 8.36 (d, *J* = 8.3 Hz, 2 H), 7.72 (d, *J* = 8.2 Hz, 2 H), 7.50 (s, 2 H), 6.45 (s, 1 H), 5.80 (s, 1 H), 5.18 (s, 1 H), 4.26 (q, *J* = 15.6 Hz, 2 H). ^{13}C NMR (101 MHz, DMSO-d_6) δ $_{ppm}$: 169.5, 168.3, 159.3, 147.9, 147.7, 147.1, 136.6, 129.3, 124.1, 118.9, 111.5, 59.0, 54.6, 18.5.

2. -Amino-6-(hydroxymethyl)-4-(4-hydroxyphenyl)-8-oxo-4,8-dihydropyrano[3,2-*b*] pyran-3-carbonitrile (7g)

White solid; Mp: > 300 °C; IR (KBr): υ (cm^{-1}) = 3422, 3350, 3268, 3032, 2923, 2200, 1685, 1657, 1631; ^{1}H NMR (400 MHz, DMSO-d_6) δ $_{ppm}$: 9.56 (s, 1 H), 7.22 (s, 2 H), 7.11 (d, *J* = 8.6 Hz, 2 H), 6.80 (d, *J* = 8.5 Hz, 2 H), 6.36 (s, 1 H), 5.74 (s, 1 H), 4.69 (s, 1 H), 4.26 (d, *J* = 15.9 Hz, 1 H), 4.17 (d, *J* = 15.8 Hz, 1 H). ^{13}C NMR (101 MHz, DMSO-d_6) δ $_{ppm}$: 169.6, 168.1, 159.1, 157.0, 149.5, 136.0, 131.1, 128.8, 119.4, 115.6, 111.2, 59.1, 56.0, 39.5.

2. -amino-4-(3-ethoxy-4-hydroxyphenyl)-6-(hydroxymethyl)-8-oxo-4,8-dihydropyrano[3,2-*b*] pyran-3-carbonitrile (7h)

^{1}H NMR (400 MHz, DMSO-d_6) δ $_{ppm}$: 9.03 (s, 1 H), 7.19 (s, 2 H), 6.80 (d, *J* = 2.0 Hz, 1 H), 6.78 (d, *J* = 8.1 Hz, 1 H), 6.64 (dd, *J* = 8.1, 2.0 Hz, 1 H), 6.32 (s, 1 H), 5.71 (t, *J* = 6.1 Hz, 1 H), 4.66 (s, 1 H), 4.19 (qd, *J* = 16.1, 6.0 Hz, 2 H), 4.00 (q, *J* = 7.0 Hz, 2 H), 1.32 (t, *J* = 7.0 Hz, 3 H). ^{13}C NMR (101 MHz, DMSO-d_6) δ $_{ppm}$: 169.5, 168.1, 159.1, 149.3, 146.7, 146.4, 136.0, 131.5, 120.0, 119.4, 115.8, 113.1, 111.2, 63.8, 59.1, 55.8, 39.8, 14.6.

Ethyl 6-amino-5-cyano-4-(4-nitrophenyl)-2-phenyl-4H-pyran-3-carboxylate (8e)

^{1}H NMR (300 MHz, DMSO-d_6) δ $_{ppm}$: 8.25 (d, *J* = 8.2 Hz, 2 H), 7.58 (d, *J* = 8.2 Hz, 2 H), 7.48 (s, 5 H), 7.20 (s, 1 H), 4.65 (s, 1 H), 3.76 (q, *J* = 7.1 Hz, 2 H), 0.73 (t, *J* = 6.9 Hz, 3 H). ^{13}C NMR (75 MHz, DMSO-d_6) δ $_{ppm}$: 165.6, 159.8, 155.0, 152.2, 147.1, 133.3, 130.5, 129.2, 129.0,

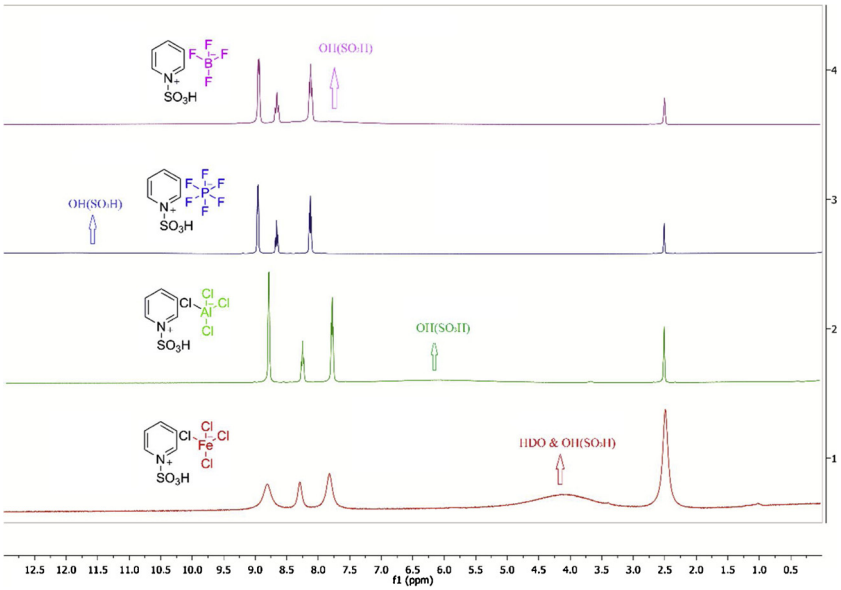

Fig. 2. ^{1}HNMR of [PySO$_3$H]X (X = BF_4, PF_6, $AlCl_4$ or $FeCl_4$) in DMSO-d_6.

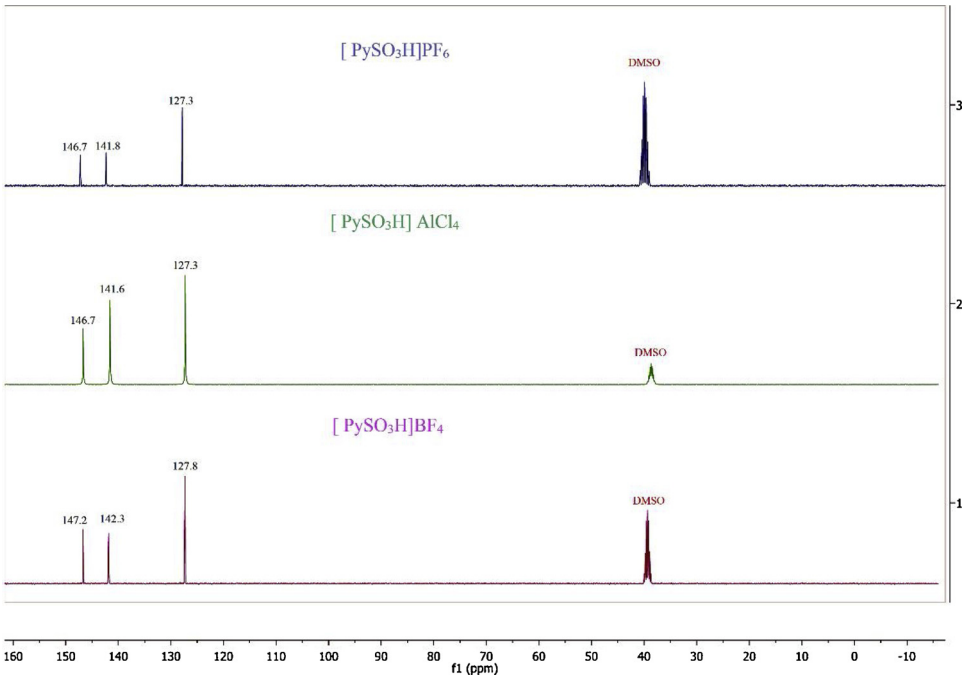

Fig. 3. ^{13}C NMR of [PySO$_3$H]X (X = BF_4, PF_6 or $AlCl_4$) in DMSO-d_6.

128.5, 127.6, 126.5, 124.4, 108.2, 60.8, 52.2, 25.0, 13.6.

Ethyl 6-amino-5-cyano-4-(3,5-difluorophenyl)-2-phenyl-4H-pyran-3-carboxylate (8 h)

White solid; Mp: 182–183 °C; IR (KBr): υ (cm^{-1}) = 3411, 3332, 3268, 3226, 2983, 2201, 1702, 1678; ^{1}H NMR (400 MHz, DMSO-d_6) δ $_{ppm}$: 7.51 - 7.43 (m, 5 H), 7.17 (d, J = 3.5 Hz, 2 H), 7.14 (td, J = 9.2, 2.4 Hz, 1 H), 7.00 (dd, J = 8.3, 2.2 Hz, 2 H), 4.57 (s, 1 H), 3.79 (qd, J = 7.1, 1.0 Hz, 2 H), 0.75 (t, J = 7.1 Hz, 3 H). ^{13}C NMR (101 MHz, DMSO-d_6) δ $_{ppm}$: 165.2, 163.6, 163.5, 161.2, 161.0, 159.1, 159.1, 155.0, 155.0, 148.9, 148.8, 148.7, 132.8, 129.9, 128.5, 127.9, 119.2, 119.2, 110.6, 110.6, 110.4, 110.4, 107.6, 102.9, 102.6, 102.3, 60.2, 55.9, 39.3, 13.1.

Ethyl 6-amino-5-cyano-4-(3-ethoxy-4-hydroxyphenyl)-2-phenyl-4H-pyran-3-carboxylate (8i)

White solid; Mp: 209–211 °C; IR (KBr): υ (cm^{-1}) = 3471, 3387, 3325, 3160, 2979, 2201, 1676; ^{1}H NMR (400 MHz, DMSO-d_6) δ $_{ppm}$: 8.86 (s, 1 H), 7.50 - 7.39 (m, 5 H), 6.94 (s, 2 H), 6.78 - 6.71 (m, 2 H), 6.64 (dd, J = 8.1, 2.0 Hz, 1 H), 4.33 (s, 1 H), 3.99 (q, J = 7.0 Hz, 2 H), 3.77 (q, J = 7.1 Hz, 2 H), 1.32 (t, J = 7.0 Hz, 3 H), 0.75 (t, J = 7.1 Hz, 3 H). ^{13}C NMR (101 MHz, DMSO-d_6) δ $_{ppm}$: 165.7, 159.0, 153.2, 146.3, 145.9, 134.9, 133.1, 129.8, 128.3, 128.0, 119.8, 119.7, 115.6, 112.9, 109.4, 63.8, 60.1, 57.2, 39.3, 14.7, 13.2.

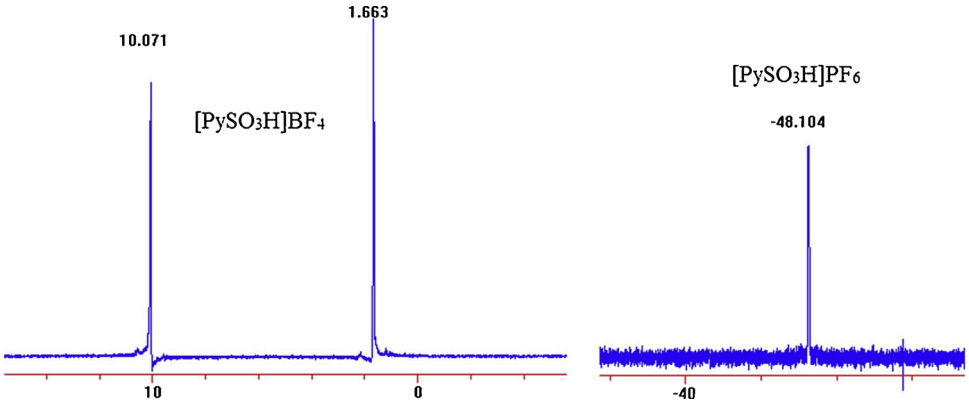

Fig. 4. ^{19}F NMR of $[PySO_3H]X$ (X = BF_4 and PF_6) in D_2O.

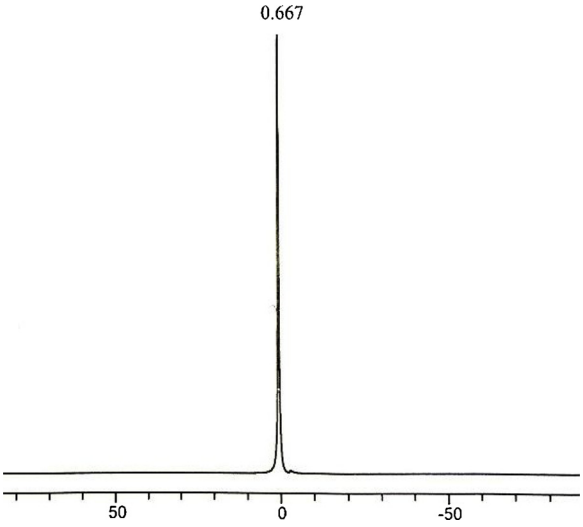

Fig. 5. ^{27}Al NMR of $[PySO_3H]AlCl_4$ in DMSO-d_6.

Ethyl 6-amino-5-cyano-2-phenyl-4-(pyridin-3-yl)-4H-pyran-3-carboxylate (8 j)

White solid; Mp: 200–201 °C; IR (KBr): υ (cm^{-1}) = 3357, 3299, 2987, 2189, 1711, 1678, 1614; ^1H NMR (400 MHz, DMSO-d_6) δ_{ppm}: 8.48 (dd, J = 6.2, 1.5 Hz, 2 H), 7.69 (dt, J = 7.9, 1.9 Hz, 1 H), 7.44 (qq, J = 7.7, 3.8, 3.0 Hz, 6 H), 7.14 (s, 2 H), 4.52 (s, 1 H), 3.76 (q, J = 6.8 Hz, 2 H), 0.72 (t, J = 7.1 Hz, 3 H). ^{13}C NMR (101 MHz, DMSO-d_6) δ_{ppm}: 165.2, 159.2, 155.0, 148.6, 148.3, 139.6, 135.0, 132.9, 130.0, 128.5, 128.0, 124.0, 119.4, 107.9, 60.2, 56.3, 37.4, 13.1.

Ethyl 6-amino-5-cyano-2-phenyl-4-(4-(trifluoromethyl)phenyl)-4H-pyran-3-carboxylate (8k)

White solid; Mp: 162–163 °C; IR (KBr): υ (cm^{-1}) = 3416, 3331, 3231, 2981, 2199, 1656, 1329; ^1H NMR (400 MHz, DMSO-d_6) δ_{ppm}: 7.74 (d, J = 8.1 Hz, 2 H), 7.54 - 7.40 (m, 7 H), 7.15 (s, 2 H), 4.57 (s, 1 H), 3.76 (q, J = 7.1 Hz, 2 H), 0.71 (t, J = 7.1 Hz, 3 H). ^{13}C NMR (101 MHz, DMSO-d_6) δ_{ppm}: 165.2, 159.2, 155.0, 148.8, 132.9, 130.0, 128.5, 128.2, 128.0, 127.8, 127.5, 127.2, 125.6, 125.6, 125.6, 125.5, 122.9, 119.4, 108.0, 60.2, 56.2, 39.6, 13.1.

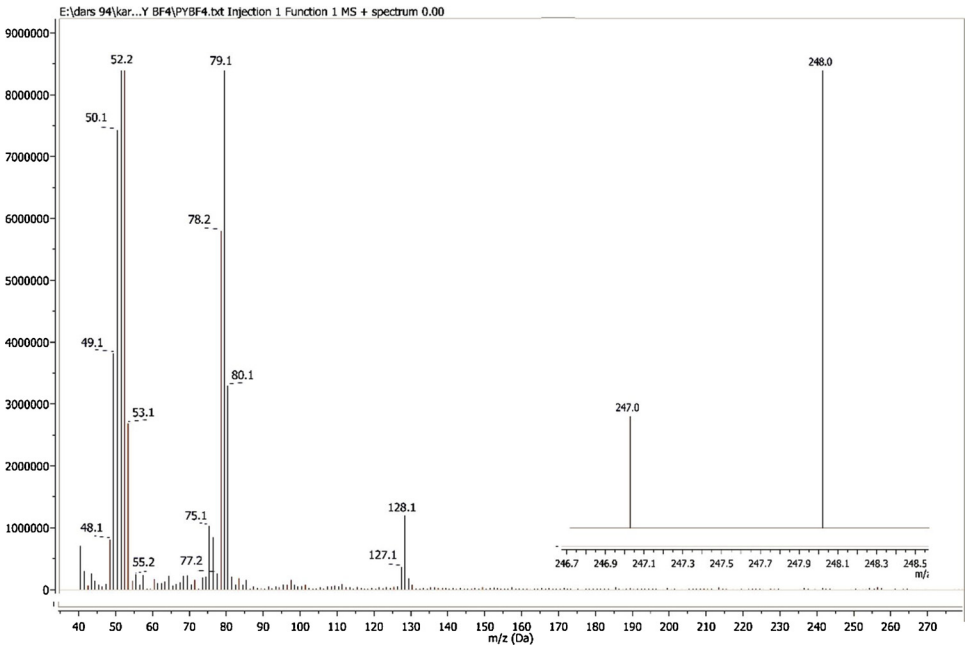

Fig. 6. Mass spectra of $[PySO_3H]BF_4$.

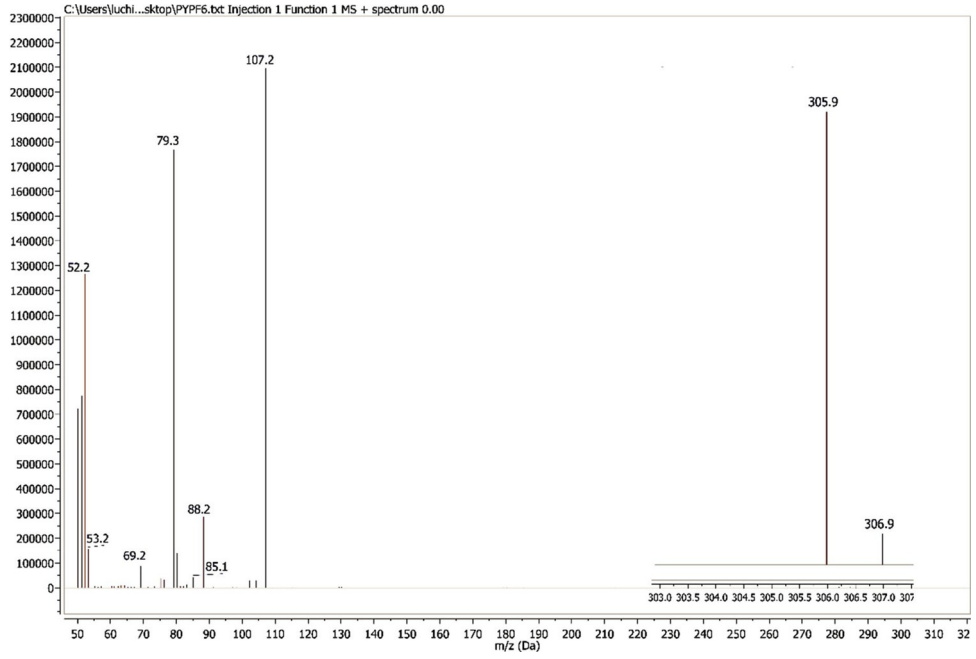

Fig. 7. Mass spectra of $[PySO_3H]PF_6$.

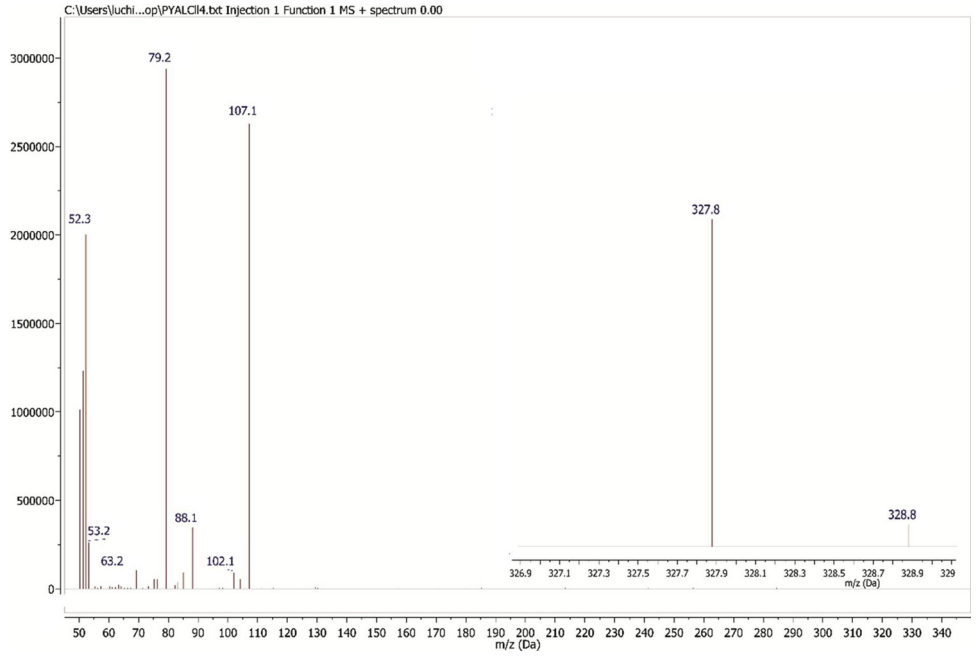

Fig. 8. Mass spectra of $[PySO_3H]AlCl_4$.

Table 1
XRD data $[PySO_3H]BF_4$.

Entry	2Θ	Peak width (degree)	Size [nm]	Inter planer distance [nm]
1	26.35	0.15	54.49	0.338
2	27.47	0.18	45.89	0.325
3	32.04	0.17	49.51	0.279
4	36.77	0.26	32.31	0.244
5	43.33	0.30	28.57	0.210
6	43.85	0.27	36.20	0.206

Table 2
XRD data $[PySO_3H]PF_6$.

Entry	2Θ	Peak width (degree)	Size [nm]	Inter planer distance [nm]
1	15.46	0.12	66.31	0.575
2	20.03	0.13	60.91	0.442
3	25.50	0.11	74.49	0.348
4	26.33	0.12	67.47	0.338
5	27.53	0.14	59.22	0.323
6	29.71	0.13	62.05	0.301

Table 3
XRD data $[PySO_3H]AlCl_4$.

Entry	2Θ	Peak width (degree)	Size [nm]	Inter planer distance [nm]
1	7.91	0.22	36.39	1.24
2	10.20	0.28	28.28	0.875
3	23.06	0.43	18.77	0.385
4	24.46	0.66	12.82	0.365

Table 4
XRD data $[PySO_3H]FeCl_4$.

Entry	2Θ	Peak width (degree)	Size [nm]	Inter planer distance [nm]
1	18.97	0.65	12.20	0.466
2	22.52	0.70	11.49	0.393
3	24.57	0.60	13.45	0.361
4	25.57	0.48	16.84	0.351
5	27.12	0.5	16.23	0.328

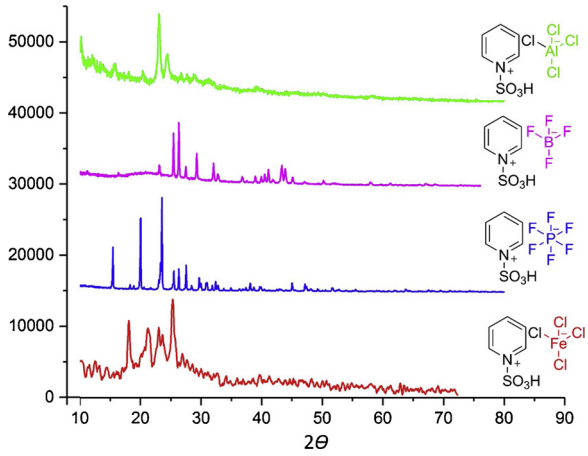

Fig. 9. XRD of $[PySO_3H]X$ (X = $AlCl_4$, BF_4, PF_6 and $FeCl_4$).

Ethyl 6-amino-5-cyano-4-(3,4-difluorophenyl)-2-phenyl-4H-pyran-3-carboxylate (8 l)

White solid; Mp: 185–187 °C; IR (KBr): υ (cm^{-1}) = 3411, 3332, 3295, 2983, 2202; ^{1}H NMR (400 MHz, DMSO-d_6) δ $_{ppm}$: 7.52 - 7.38 (m, 6 H), 7.32 (ddd, J = 11.5, 7.7, 2.2 Hz, 1 H), 7.11 (s, 3 H), 4.51 (s, 1 H), 3.77 (qd, J = 7.2, 1.0 Hz, 2 H), 0.73 (t, J =7.1 Hz, 3 H). ^{13}C NMR (101 MHz, DMSO-d_6) δ $_{ppm}$: 165.3, 159.1, 154.6, 150.5, 150.4, 149.71, 149.6, 148.1, 148.0, 147.3, 147.1, 142.0, 142.0, 141.9, 132.9, 129.9, 128.5, 128.0, 124.2, 124.2, 124.1, 124.1, 119.4, 117.7, 117.5, 116.5, 116.3, 108.1, 60.2, 56.3, 39.5, 13.2.

Ethyl 6-amino-4-(3,5-bis(trifluoromethyl)phenyl)-5-cyano-2-phenyl-4H-pyran-3-carboxylate (8 m)

White solid; Mp: 185–187 °C; IR (KBr): υ (cm^{-1}) = 3410, 3323, 3294, 3207, 2982, 2201, 1680, 1612; ^{1}H NMR (400 MHz, DMSO-d_6) δ $_{ppm}$: 8.06 (s, 1 H), 7.95 (s, 2 H), 7.51 - 7.43 (m, 5 H), 7.26 (s, 2 H), 4.84 (s, 1 H), 3.75 (qd, J = 7.1, 1.0 Hz, 2 H), 0.71 (t, J =7.1 Hz, 3 H). ^{13}C NMR (101 MHz, DMSO-d_6) δ $_{ppm}$: 165.2, 159.3, 155.2, 147.8, 132.6, 130.9, 130.6, 130.3, 130.2, 130.0, 128.4, 128.1, 127.3, 124.6, 121.9, 119.1, 107.3, 60.3, 55.6, 39.1, 13.0.

Result and discussion

As mentioned above, the ionic liquid $[PySO_3H]BF_4$ and molten salts $[PySO_3H]X$ (X = $FeCl_4$, PF_6 and $AlCl_4$) were synthesized by one-pot reaction of salts ($AlCl_3$, $FeCl_3$, $NaBF_4$ or KPF_6) and $[PySO_3H]Cl$ under solvent free condition at 60 °C (Scheme 3). Then, structures of $[PySO_3H]X$ (X = $FeCl_4$, BF_4, PF_6 and $AlCl_4$) were studied using techniques FT-IR, NMR (^{1}H, ^{13}C, ^{9}F & ^{27}Al) and mass spectra. In the following, morphological and dimensions of the presented IL and MSs were studied by using of XRD and SEM techniques. Furthermore, TG, DTG and DTA analysis were used for showing the range of their corresponding thermal stability of $[PySO_3H]X$ (X = $FeCl_4$, BF_4, PF_6 and $AlCl_4$).

The FT-IR spectrum of $[PySO_3H]Cl$ and $[PySO_3H]X$ (X = $FeCl_4$, BF_4, PF_6 and $AlCl_4$) were compared in Fig. 1. FT-IR of the all of the mentioned IL and MSs catalyst includes the broad peak of the O—H acid groups SO_3H at 2500–3400 cm^{-1}. In addition, two peaks 1201 − 1056, 1187 − 1051, 1176 − 1071 and 1255 − 1095 cm^{-1} have a good correlation with vibrational transplantation of O—S and N—S respectively (Fig. 1). Hexafluorophosphate $[Py\text{-}SO_3H]PF_6$ was shown a broad strong band at 834 cm^{-1} [39] and tetrafluoroborat $[Py\text{-}SO_3H]BF_4$ shown broad band at 1086 cm^{-1} [40]. The O—H stretching regions in FT-IR (Fig. 1) are different among for different presented catalysts which are due to the presence of fluorine within the structure of both of them. These differences may be due to the intra-molecular hydrogen bonding between hydrogen of SO_3H group with the fluorine of their corresponding counter ions in the structure of two catalysts $[PySO_3H]X$ (X = BF_4, PF_6).

The spectra of NMR (^{1}H, ^{13}C, ^{19}F & ^{27}Al in DMSO-d_6 and D_2O) $[PySO_3H]X$ (X = BF_4, PF_6, $AlCl_4$ and $FeCl_4$) was performed the

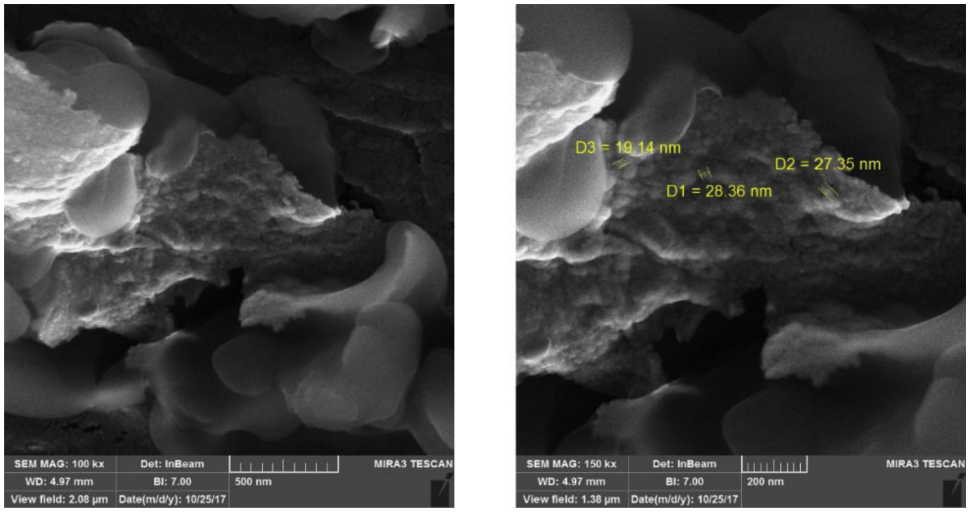

Fig. 10. SEM of $[PySO_3H]BF_4$.

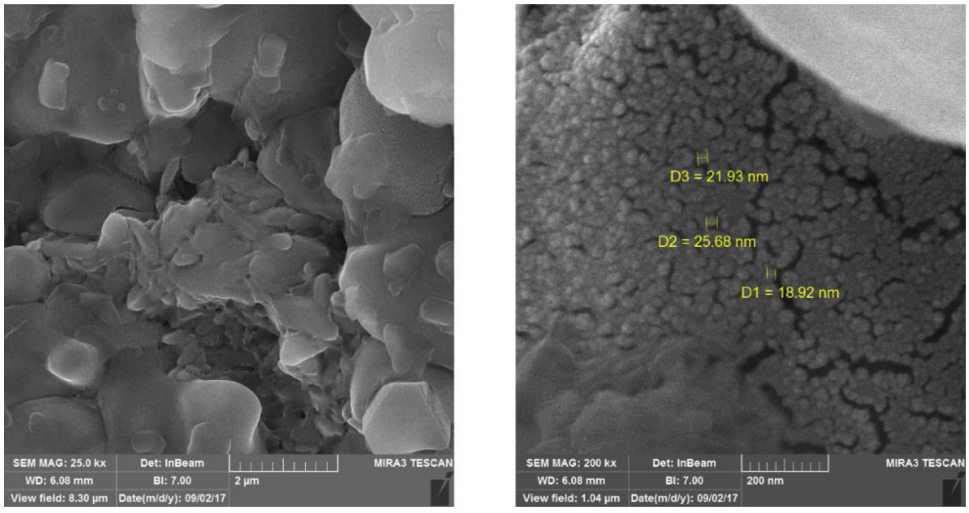

Fig. 11. SEM of $[PySO_3H]PF_6$.

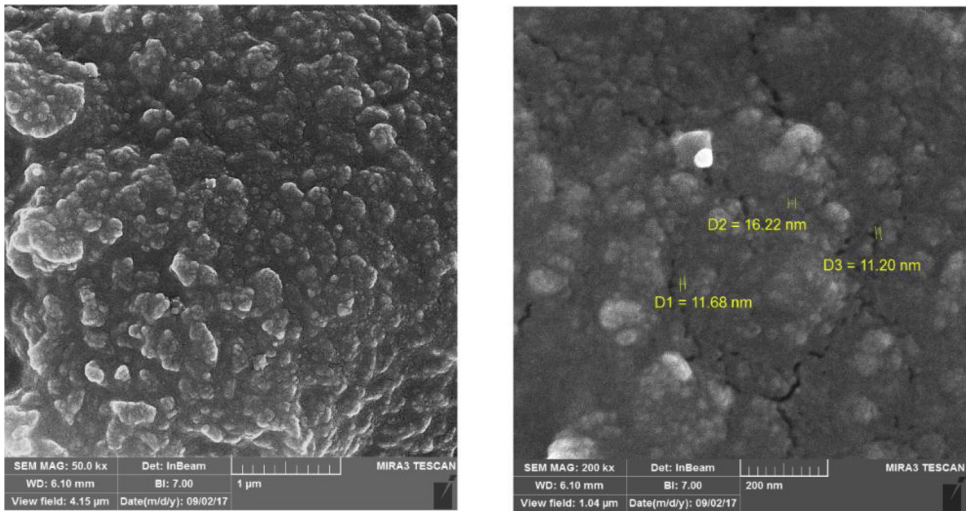

Fig. 12. SEM of $[PySO_3H]AlCl_4$.

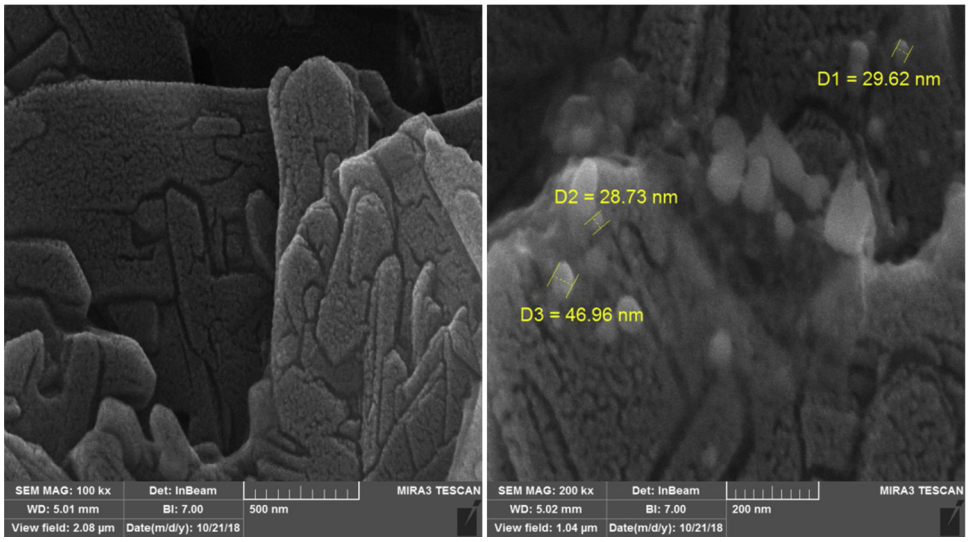

Fig. 13. SEM of $[PySO_3H]FeCl_4$.

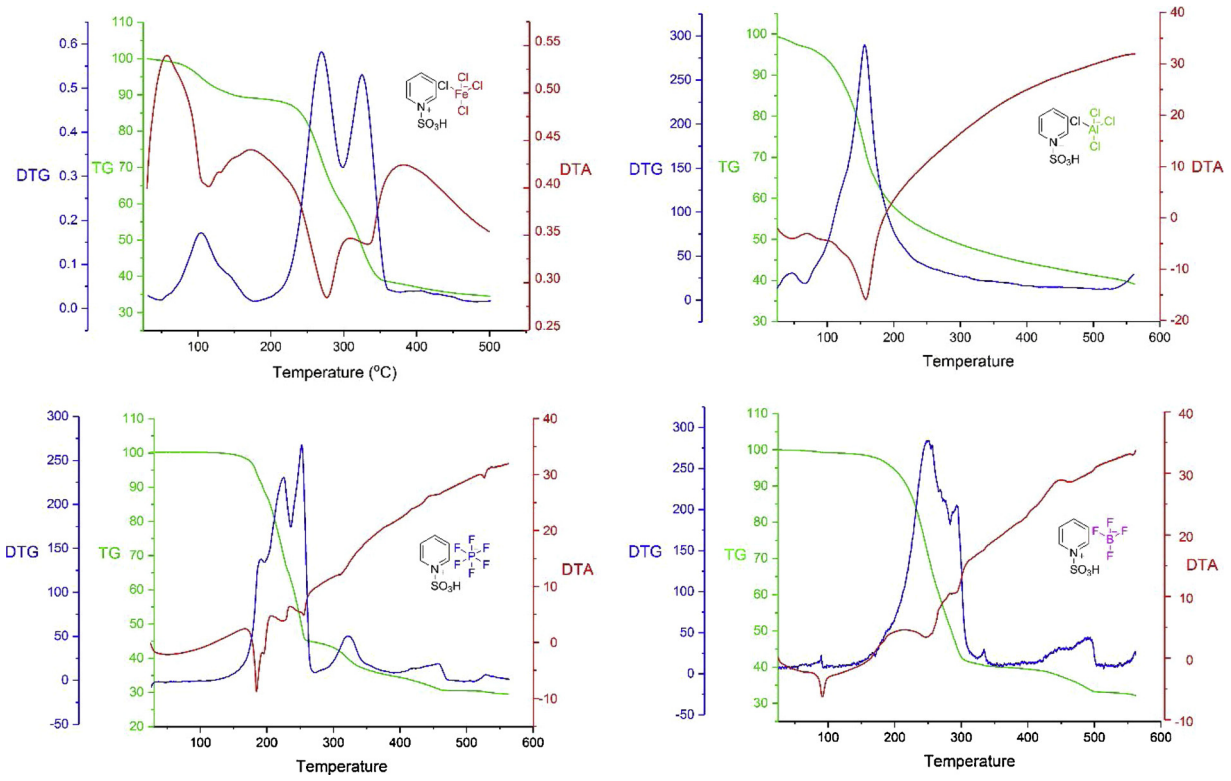

Fig. 14. TG, DTG and DTA analysis of the synthesized [$PySO_3H$]X.

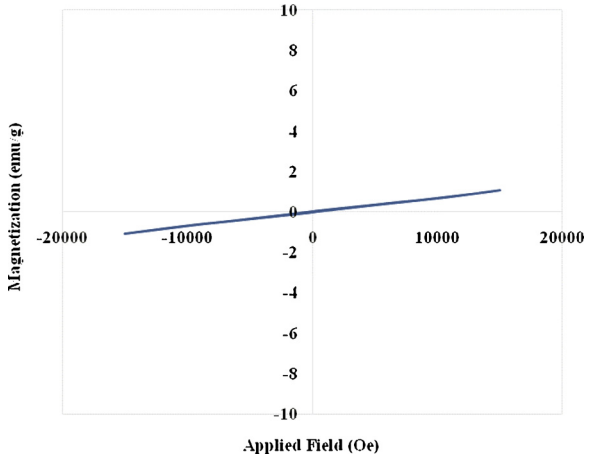

Fig. 15. The vibrating sample magnetometer (VSM) of [$PySO_3H$]$FeCl_4$.

structure of catalyst. The spectra of ^{1}H NMR (400 MHz) shows O—H peak of acid groups (SO_3H) at δ $_{ppm}$: 7.88 (s, 1H, OH), 11.91 (s, 1H, OH), 10.68 (s, 1H, OH) and 4.10 (s, 1H, OH) related to [$PySO_3H$]X (X = BF_4, PF_6, $AlCl_4$ and $FeCl_4$) respectively (Fig. 2). Peak of C—H aromatic related to [$PySO_3H$]BF_4 δ $_{ppm}$: 8.94 (d, J = 5.6 Hz, 2 H), 8.66 (t, J = 7.9 Hz, 1 H), 8.12 (t, J = 6.9 Hz, 2 H), [$PySO_3H$]PF_6: δ $_{ppm}$: 8.96 (d, J = 5.3 Hz, 2 H), 8.66 (t, J = 7.8 Hz, 1 H), 8.12 (t, J = 6.9 Hz, 2 H), [$PySO_3H$]$AlCl_4$: δ $_{ppm}$: 8.63 (d, J = 4.8 Hz, 2 H), 7.90 (td, J = 7.7, 3.8 Hz, 1 H), 7.48 (dd, J = 7.9, 5.3 Hz, 2 H) and [$PySO_3H$]$FeCl_4$: δ $_{ppm}$: 8.81 (s, 2 H), 8.29 (s, 1 H), 7.82 (s, 2 H) (Fig. 2). The ^{1}H NMR analysis changes of [$PySO_3H$]Cl in comparison with [$PySO_3H$]X displayed the synthesis of [$PySO_3H$]X.

The spectra of ^{13}C NMR (101 MHz, DMSO-d_6) of the above said ILs and MSs [$PySO_3H$]X (X = BF_4, PF_6 or $AlCl_4$) were compared in Fig. 3. Peaks C = C of pyridine (δ $_{ppm}$: 147.2, 142.3, 127.8), (δ $_{ppm}$: 146.7, 141.8, 127.3) and (δ $_{ppm}$: 146.7, 141.6, 127.3) were related to [$PySO_3H$]BF_4, [$PySO_3H$]PF_6 and [$PySO_3H$]$AlCl_4$ respectively. Also, peaks (s, -48.10) and (d, 10.07, 1.663, J = 756.72 Hz) of [$PySO_3H$]BF_4 and [$PySO_3H$]PF_6 were related to ^{19}F NMR (84 MHz, D_2O), respectively (Fig. 4). Furthermore, the spectra of ^{27}Al NMR (26 MHz, DMSO-d_6) of [$PySO_3H$]$AlCl_4$ was observed a peak at δ $_{ppm}$ 0.667 (Fig. 5). In continued, MS m/z (%); found for [$PySO_3H$]BF_4: 247.0, [$PySO_3H$]PF_6: 305.9, [$PySO_3H$]$AlCl_4$: 327.8 in Figs. 6–8 respectively.

The particle size and shape as well as the morphology of [$PySO_3H$]X (X = $FeCl_4$, BF_4, PF_6 and $AlCl_4$) were studied by XRD (Tables 1–4 and Fig. 9) and SEM (Figs. 10–13). Characterization was performed by X-ray diffraction (XRD) crystalline structure of [$PySO_3H$]X using the technique XRD (Fig. 9) and calculations Debye-Sherrer equation D = Kλ/βcosθ and Bragg equation: dhkl = λ/(2sinθ) (Tables 1–4). The size of the catalysts is in the range of [$PySO_3H$]BF_4: 28.57–54.45 nm (Table 1), [$PySO_3H$]PF_6: 59.22–84.03 nm (Table 2),[$PySO_3H$]$AlCl_4$: 12.82–36.39 nm (Table 3) and [$PySO_3H$]$FeCl_4$: 11–16 nm (Table 4). The scanning electron microscope (SEM) micrographs of the catalysts also showed that the particles of [$PySO_3H$]X (X = $FeCl_4$, BF_4, PF_6 or $AlCl_4$) that their structures were observed in scale and not completely agglomerated respectively (Figs. 10–13).

To study the thermal stability of presented IL and MSs the thermal gravimetric (TG), derivative thermal gravimetric (DTG) and differential thermal (DTA) analysis were performed. Several degradation stages were observed for [$PySO_3H$]X (X = BF_4, PF_6, $AlCl_4$ and $FeCl_4$) in their obtained profiles patterns (Fig. 14). The first step is the weight loss, taking place between 25 and 100 °C associated with the removal of organic solvents which have been used in the course of their preparation. The main stage of weight loss was related to SO_3H release due to breaking of N—S bond structure of [$PySO_3H$]X. Therefore, about 60%, 50%, 30%, and 50% for [$PySO_3H$]BF_4, [$PySO_3H$]PF_6, [$PySO_3H$]$AlCl_4$, and [$PySO_3H$]$FeCl_4$ respectively weight loss were observed. [$PySO_3H$]X (BF_4, PF_6, $AlCl_4$ and $FeCl_4$) can be used up to about 250, 211, 160 and 268 °C respectively.

In another investigation, magnetic measurements of [$PySO_3H$]$FeCl_4$ was investigated at room temperature by using a vibrating sample

Table 5
Effect of different amounts of catalysts, temperature and solvent (5 ml) in the synthesis of 4*H*-benzo[g]chromene.

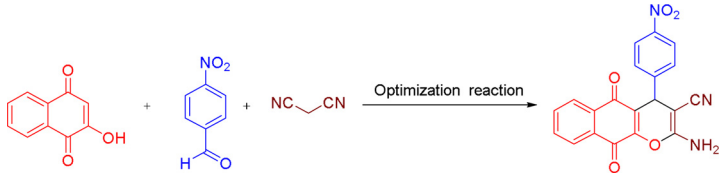

Entry	Catalyst (mol%) ($[PySO_3H]FeCl_4$)	Temp. (°C)	Solvent	Time (min)	Yield (%)
1	–	90	–	120	Trace
2	5	90	–	50	67
3	7	90	–	35	79
4	10	90	–	20	90
5	10	90	–	20	90
6	15	90	–	20	88
7	20	90	–	20	88
8	10	110	–	20	89
9	10	70	–	35	74
10	10	50	–	40	71
11	10	r.t.	–	65	67
12	10	Reflux	H_2O	35	71
13	10	Reflux	EtOH	30	81
14	10	Reflux	CH_3CN	30	80
15	10	Reflux	*n*-Hexane	90	–
16	10	Reflux	EtOAc	60	30

Reaction conditions: 4-nitrobenzaldehyde (1 mmol, 0.151 g), malononitrile (1 mmol, 0.066 g) and 2-hydroxynaphtalen-1,4-dione (1 mmol, 0.174 g).

Table 6
Synthesis of 4*H*-benzo[g]chromene using $[PySO_3H]X$ (X = BF_4, PF_6, $AlCl_4$ and $FeCl_4$) at 90 °C. (a: $[PySO_3H]FeCl_4$, b: $[PySO_3H]AlCl_4$, c: $[PySO_3H]PF_6$ and d:$[PySO_3H]BF_4$)[41–44].

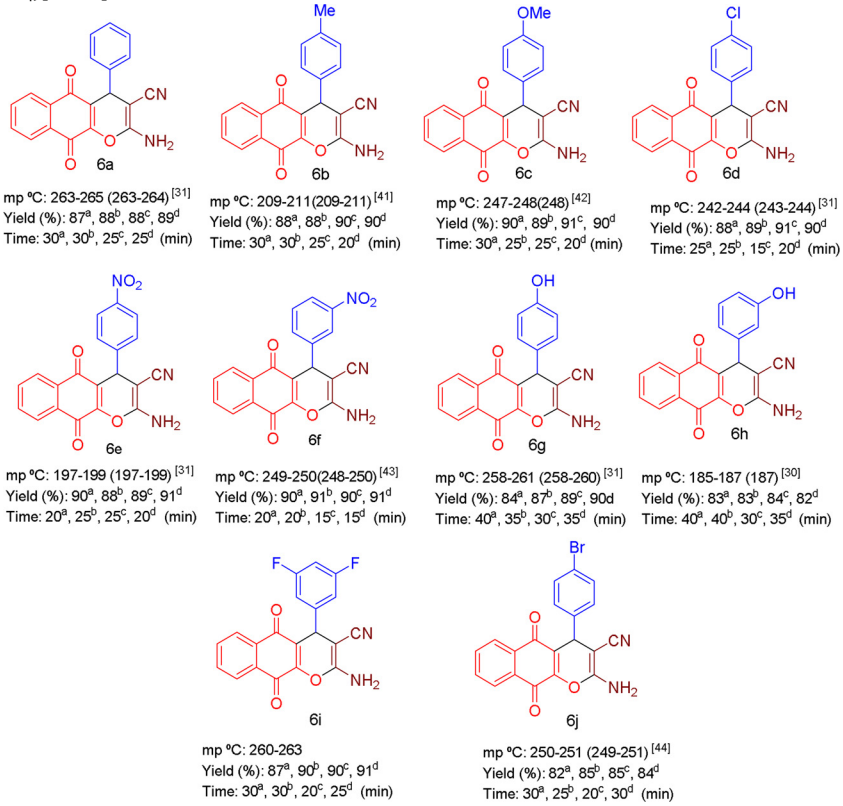

magnetometer (VSM) in Fig. 15. Based on magnetization curves, the saturation of the obtained catalyst dropped to 2.2 emu g^{-1}. Therefore, this amount of magnetic ability is not enough for isolating of $[PySO_3H]FeCl_4$ as a catalyst from the reaction mixture by using an external magnet. This low paramagnetic property is due to decreasing of the five unpaired electrons of Fe^{3+} to one unpaired electron via addition of a chloride (Cl^-) ligand to it and formation of $FeCl_4^-$ counter ion.

After the synthesis and full characterization of $[PySO_3H]BF_4$, $[PySO_3H]PF_6$, $[PySO_3H]AlCl_4$ and $[PySO_3H]FeCl_4$ as catalysts, they were used for the synthesis of *O*-heterocyclic compounds (2-amino-4*H*-

Table 7
Synthesis of 2-amino-4,8-dihydropyrano using [$PySO_3H$]X (X = BF_4, PF_6, $AlCl_4$ and $FeCl_4$) at 90 °C.(a: [$PySO_3H$]$FeCl_4$, b: [$PySO_3H$]$AlCl_4$, c: [$PySO_3H$]PF_6 and d: [$PySO_3H$]BF_4)[45–47].

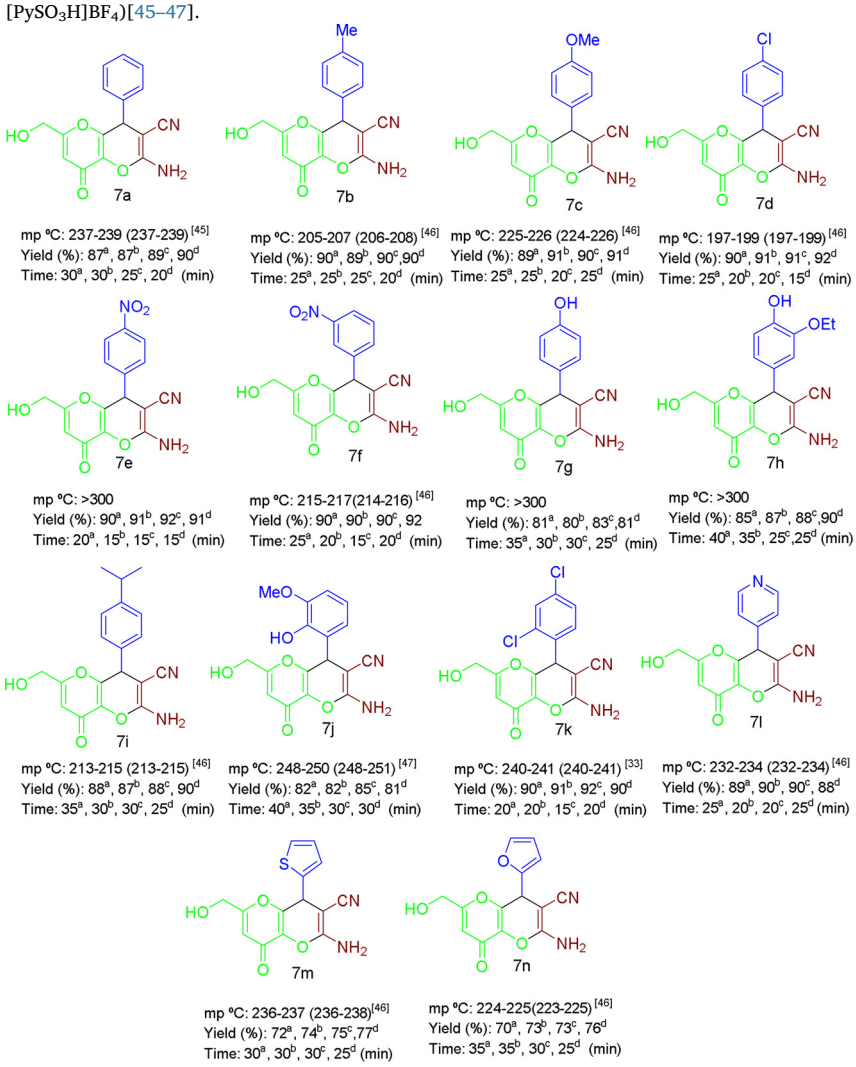

chromene, 2-amino-4,8-dihydropyrano and 2-amino-4*H*-pyrans). The mentioned *O*-heterocyclic derivatives were synthesized *via* a condensation reaction of suitable starting materials in the presence of [$PySO_3H$]X (X = BF_4, PF_6, $AlCl_4$ and $FeCl_4$). The condensation of 4-nitrobenzaldehyde (1 mmol, 0.151 g), malononitrile (1 mmol, 0.066 g) and 2-hydroxynaphtalen-1,4-dione (1 mmol, 0.174 g) was selected as model reaction to optimize the reaction conditions. As shown in the Table 5, the worthy results were obtained when the reaction was achieved in the presence of 10 mol% of MSs {[$PySO_3H$]$FeCl_4$ (Table 5, entry 5). No improvement was detected in the yield of the reaction using different amounts of the catalyst and temperature (Table 5, entries 2-3 and entries 6-11). Table 5 clearly displayed that in the absence of catalyst the product was produced in a low yield (Table 5, entry 1). To investigate the solvent effect on the reaction improvement, several solvents such as solvent free, H_2O, EtOH, CH_3CN, *n*-hexane and EtOAc (5 ml) were tested and compared with solvent free condition in the presence of 10 mol% [$PySO_3H$]$FeCl_4$ (Table 5, entries 12-16). The results are summarized in Table 5.

In continuation of our investigations on the scope and limitations of IL and MSs their efficiency and applicability the reaction of malononitrile (1 mmol, 0.066 g), *O*-compounds (5-Hydroxy-2-(hydroxymethyl)-4H-pyran-4-one, 2-hydroxynaphtalen-1,4-dione and ethyl benzoylacetate) (1 mmol) and various aryl aldehydes such as electron-withdrawing and electron-releasing substituents were checked out. As exposed in the Tables 6–8, the results show that the described methodologies are suitable for the synthesis of a range of *O*-heterocyclic derivatives such as 2-amino-4*H*-chromene, 2-amino-4,8-dihydropyrano and 2-amino-4*H*-pyrans in high to excellent yields (70–93%) with in relatively short reaction times (15–50 min). The results of this study shows that aldehydes which have electron withdrawing groups to produce the desired products with high yields and low reaction times in compared to the electron releasing ones.

Suggested mechanism for the synthesis *O*-heterocyclic derivatives (2-amino-4*H*-chromene, 2-amino-4,8-dihydropyrano and 2-amino-4*H*-pyrans) using described catalysts [$PySO_3H$]X (X = BF_4, PF_6, $AlCl_4$ or $FeCl_4$) have been summarized in Scheme 5. Initially aldehyde is activated by the acidic sites of the catalyst, in which malononitrile is reacted with aldehyde by removing one water molecule, to afford intermediate (**I**). For approving the formation of complex A, 4-nitro benzaldehyde was reacted with [$PySO_3H$]X (X = BF_4, PF_6, $AlCl_4$ or $FeCl_4$) at room temperature. Then the FT-IR spectra of the reaction mixtures were examined: The absorption bond of C=O of the 4-nitro benzaldehyde at the 1703 cm^{-1} was changed to 1708, 1708, 1707 and 1708 cm^{-1} for the complex A respectively (Fig. 16) [49]. Then, intermediate (**I**) as Michael acceptor to react with nucleophilic substrate (2-hydroxynaphtalen-1,4-dione, 5-hydroxy-2-(hydroxymethyl)-4*H*-pyran-4-one or ethyl benzoylacetate) to afford intermediate (**II**). Finally, intermediate (**II**) after intramolecular cyclization and tautomerization to

Table 8
Synthesis of 2-amino-4*H*-pyrans using $[PySO_3H]X$ (X = BF_4, PF_6, $AlCl_4$ and $FeCl_4$) at 90 °C. (a: $[PySO_3H]FeCl_4$, b: $[PySO_3H]AlCl_4$, c: $[PySO_3H]PF_6$ and d:$[PySO_3H]BF_4$)[48, 49].

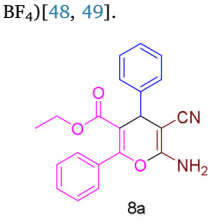

mp °C: 185-187 (188) [43]
Yield (%): 82[a], 83[b], 83[c], 85[d]
Time: 45[a], 45[b], 35[c], 35[d] (min)

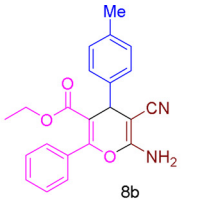

mp °C: 146-148 (146-148) [35]
Yield (%): 84[a], 84[b], 85[c], 90d
Time: 40[a], 35[b], 35[c], 30[d] (min)

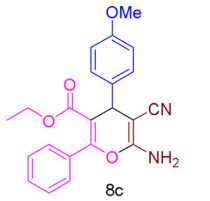

mp °C: 151-152 (150-152) [35]
Yield (%): 84[a], 85[b], 85[c], 89[d]
Time: 35[a], 30[b], 30[c], 35[d] (min)

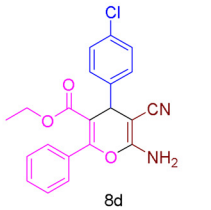

mp °C: 189-191(189-190) [49]
Yield (%): 88[a], 90[b], 90[c], 91[d]
Time: 25[a], 20[b], 20[c], 20[d] (min)

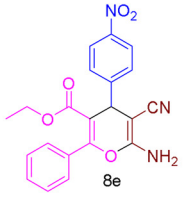

mp °C: 160-161(158-160) [35]
Yield (%): 90[a], 90[b], 91[c], 93[d]
Time: 25[a], 20[b], 15[c],15[d] (min)

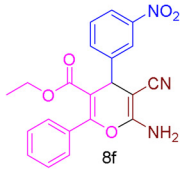

mp °C: 250-251 (251-252) [49]
Yield (%): 89[a], 90[b], 90[c],92[d]
Time: 35[a], 20[b], 20[c], 15[d] (min)

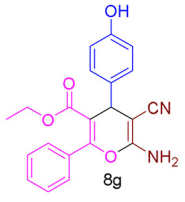

mp °C: 160-162 (160-162) [35]
Yield (%): 80[a], 81[b], 80[c], 83[d]
Time: 45[a], 45[b], 40[c], 45[d] (min)

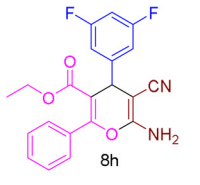

mp °C: 182-183
Yield (%): 78[a], 80[b], 81[c], 86[d]
Time: 35[a], 30[b], 30[c], 30[d](min)

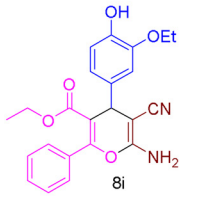

mp °C: 209-211
Yield (%): 84[a], 84[b], 87[c], 82[d]
Time: 50[a], 45[b], 45[c], 30[d] (min)

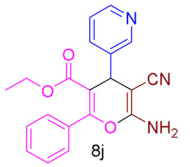

mp °C: 200-201
Yield (%): 86[a], 85[b], 88[c], 91[d]
Time: 30[a], 25[b], 25[c], 30[d] (min)

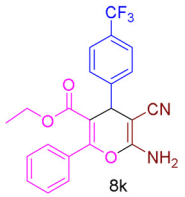

mp °C: 162-163
Yield (%): 84[a], 84[b], 87[c], 87[d]
Time: 25[a], 25[b], 25[c], 20[d] (min)

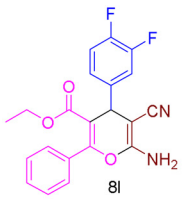

mp °C: 160-161
Yield (%): 84[a], 84[b], 87[c],85[d]
Time: 25[a], 25[b], 20[c], 20[d] (min)

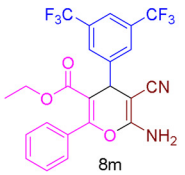

mp °C: 202-204
Yield (%): 84[a], 84[b], 87[c], 84[d]
Time: 35[a], 30[b], 30[c], 30[d] (min)

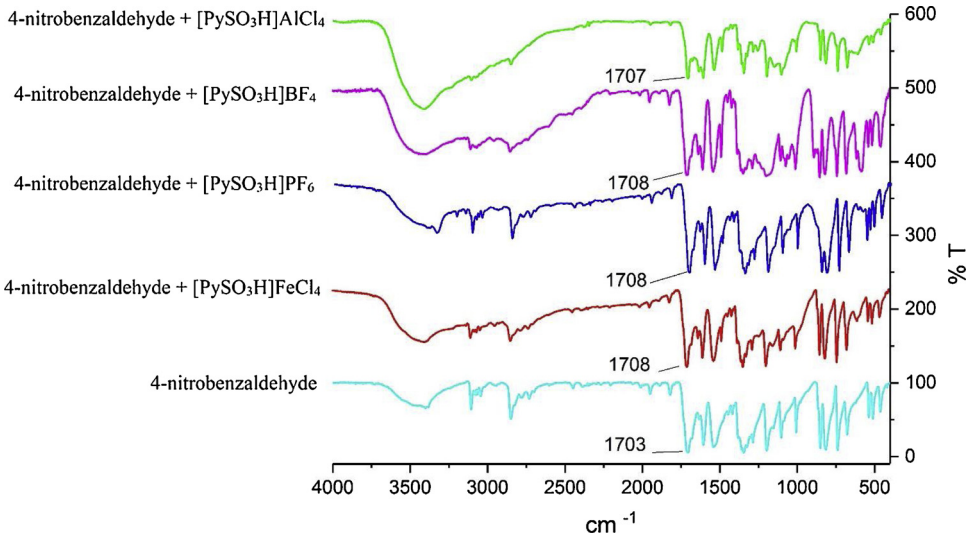

Fig. 16. FT-IR spectra of 4-nitro benzaldehyde and complex A.

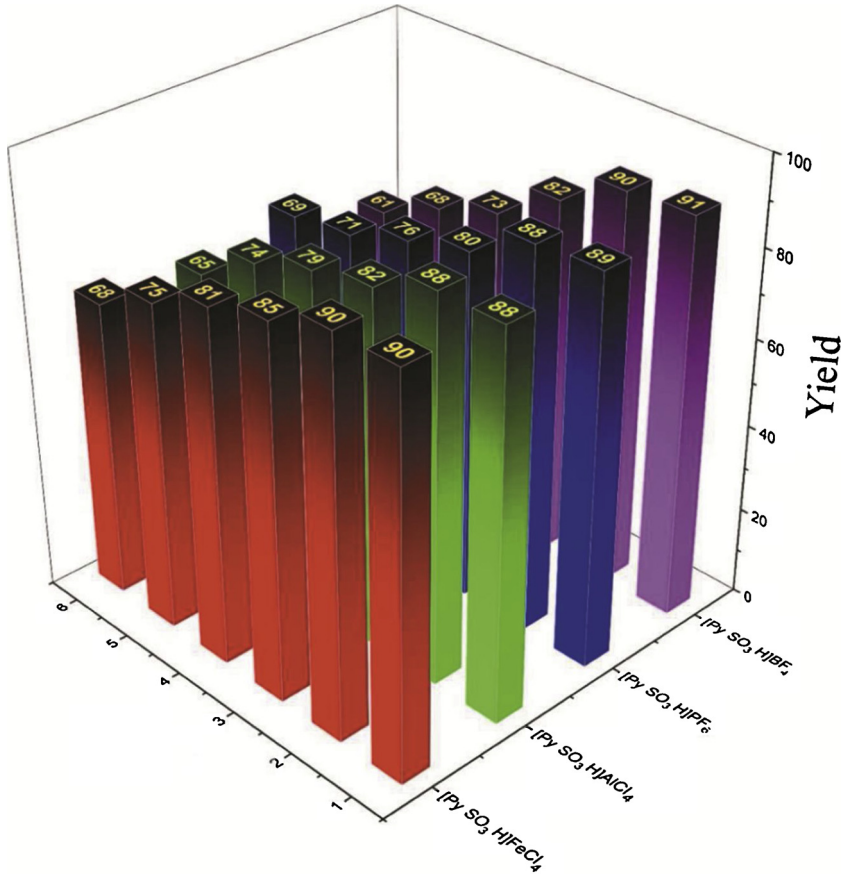

Fig. 17. Recyclability of $[PySO_3H]X$ (X = BF_4, PF_6, $AlCl_4$ or $FeCl_4$) for the synthesis *O*- heterocycle compounds.

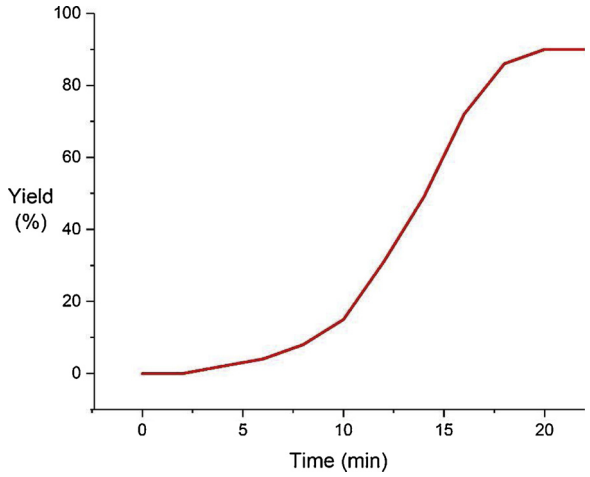

Fig. 18. Variation of the reaction conversion and yield with time in the synthesis of 4*H*-benzo[g]chromene.

give the desired corresponding *O*-heterocyclic compounds (Scheme 3).

The recyclability and reusing of the described IL and MSs were also studied on a model reaction of 4-nitrobenzaldehyde (1 mmol, 0.151 g), malononitrile (1 mmol, 0.066 g) and 2-hydroxynaphtalen-1,4-dione (1 mmol, 0.174 g) under the above mentioned optimized reaction conditions (for fixed time 20 min). As indicated in the Fig. 17, the applied IL and MSs could be recycled (see experimental for details) and efficiently reused up to five reaction cycles with a marginal decreasing their catalytic activities.

The results of catalytic tests in the solvent-free reaction of 4-nitrobenzaldehyde (1 mmol, 0.151 g), malononitrile (1 mmol, 0.066 g) and 2-hydroxynaphtalen-1,4-dione (1 mmol, 0.174 g) over $[PySO_3H]FeCl_4$ at 90 ∘C (variation of conversion or yield with time), are shown in Fig. 18. It was found that after 20 min, the reaction conversion of (1) was 90%.

To compare the efficiency of $[PySO_3H]X$ (X = BF_4, PF_6, $AlCl_4$ or $FeCl_4$) with the previously reported catalysts for the synthesis of 4*H*-benzo[g]chromene, we have tabulated the results of these catalysts to perform the condensation of 4-nitrobenzaldehyde (1 mmol, 0.151 g), malononitrile (1 mmol, 0.066 g) and 2-hydroxynaphtalen-1,4-dione (1 mmol, 0.174 g), in the Table 9. As Table 9 indicates, $[PySO_3H]X$ (X = BF_4, PF_6, $AlCl_4$ or $FeCl_4$) have remarkably improved the synthesis of 4*H*-benzo[g]chromene in different terms (reaction times and yields). The presented results of the Table 9 shows those both basic and acidic properties of applied compounds as catalysts are important for proceeding of the target reaction. For entry 8 ($NaBF_4$) due to very low Lewis acidity and basic properties, the efficiency of the reaction was seriously decreased and the reaction times are also increased.

Conclusion

In summary, we have synthesized pyridinium-based ionic liquid (IL) $[PySO_3H]PF_6$ and molten salts (MSs) such as $[PySO_3H]AlCl_4$, $[PySO_3H]BF_4$, and $[PySO_3H]FeCl_4$ via a convenient anion exchange method.

The above mentioned ILs and MSs fully characterized by using several identification techniques. These molten salts were applied for one-pot synthesis of *O*-heterocyclic compounds (2-amino-4*H*-chromene, 2-amino-4,8-dihydropyrano and 2-amino-4*H*-pyrans) under mild conditions. The mentioned molecules as biological active and drug candidates have demonstrated that medicinal properties such anti-cancer, anti-alzheimer, anti-malarial, antitumor, antioxidants and antifungal. The promising points for the described catalytic methodologies are easy work-up, recycle and reusability of the catalysts, high efficiency, short

Table 9
Comparison of the previously reported results for the synthesis of 4*H*-benzo[g]chromene with our new described catalysts.

Entry	Catalyst	Reaction condition	Time (min)	Yield (%)	Reference
1	POPINO	Reflux/ H_2O	20	91	[31]
2	MW	DMF/ HOAc	5	92	[50]
3	[bmim]OH	r.t. / EtOH	60	91	[51]
4	DBU	Reflux/ H_2O	60	87	[52]
5	Fe_3O_4/(PEG)	Ultrasonic irradiation/EtOH	20	85	[53]
6	Imidazole	Reflux/ EtOH	30	93	[45]
7	Piperidine	r.t. / EtOH	15	85	[54]
8	$[PySO_3H]Cl$	Solvent free/ 90 °C	60	56	a
9	$[PySO_3H]AlCl_4$	Solvent free/ 90 °C	30	87	a
10	$[PySO_3H]FeCl_4$	Solvent free/ 90 °C	30	88	a
11	$[PySO_3H]PF_6$	Solvent free/ 90 °C	25	88	a
12	$[PySO_3H]BF_4$	Solvent free/ 90 °C	25	89	a
13	$AlCl_3$	Solvent free/ 90 °C	45	52	a
14	$NaBF_4$	Solvent free/ 90 °C	60	Trace	a
15	$FeCl_3$	Solvent free/ 90 °C	40	65	a
16	KPF_6	Solvent free/ 90 °C	60	45	a
17	DABCO[b] + $[PySO_3H]FeCl_4$	Solvent free/ 90 °C	40	65	a

[a]Our work.
[b]1,4-diazabicyclo[2.2.2]octane.

reaction times and high yields of products. The efficacy of the above mentioned catalysts may be due to the presence both of the proton and Lewis acidic sites within their structures. Furthermore, the major advantages of anion exchange method are preparing a good range of novel molten salts $[PySO_3H]X$ (X = $FeCl_4$, $AlCl_4$, BF_4 and PF_6) as an efficient, task-specific, recyclable and thermally stable catalysts.

Acknowledgements

We thank the Bu-Ali Sina University, National Elites Foundation and Iran National Science Foundation (INSF) (Grant Number: 96013474) for financial support.

Appendix A. Supplementary data

Supplementary material related to this article can be found, in the online version, at doi:https://doi.org/10.1016/j.mcat.2019.110403.

References

[1] M.A. Zolfigol, V. Khakyzadeh, A.R. Moosavi-Zare, A. Zare, S.B. Azimi, Z. Asgari, A. Hasaninejad, C. R. Chim. 15 (2012) 719.
[2] S. Saikia, P. Gogoi, A.K. Dutta, P. Sarma, R. Borah, J. Mol. Catal. A: Chem. 416 (2016) 63.
[3] E. Muresan, S. Oprea, V. Hulea, T. Malutan, M. Vata, Open Chem. 6 (2008) 419.
[4] V. Mévellec, B. Leger, M. Mauduit, A. Roucoux, Chem. Commun. (2005) 2838.
[5] M.A. Zolfigol, A. Khazaei, A.R. Moosavi-Zare, A. Zare, V. Khakyzadeh, Appl. Catal. A Gen. 400 (2011) 70.
[6] D. Fang, H.B. Zhang, Z.L. Liu, J. Heterocycl Chem . 47 (2010) 63.
[7] M.A. Zolfigol, A. Khazaei, A.R. Moosavi-Zare, A. Zare, H.G. Kruger, Z. Asgari, V. Khakyzadeh, M. Kazem-Rostami, J. Org. Chem. 77 (2012) 3640.
[8] H. Ghaderi, M.A. Zolfigol, Y. Bayat, M. Zarei, E. Noroozizadeh, Synlett 27 (2016) 2246.
[9] A.R. Moosavi-Zare, M.A. Zolfigol, E. Noroozizadeh, Synlett 27 (2016) 1682.
[10] M. Zarei, E. Noroozizadeh, A.R. Moosavi-Zare, M.A. Zolfigol, J. Org. Chem. 83 (2018) 3645.
[11] M.A. Zolfigol, A. Khazaei, A.R. Moosavi-Zare, A. Zare, Org. Prep. Proced. Int. 42 (2010) 95.
[12] M.A. Zolfigol, H. Vahedi, S. Azimi, A.R. Moosavi-Zare, Synlett 24 (2013) 1113.
[13] A.R. Moosavi-Zare, M.A. Zolfigol, M. Daraei, Synlett 25 (2014) 1173.
[14] A. Khazaei, M.A. Zolfigol, A.R. Moosavi-Zare, Z. Asgari, M. Shekouhy, A. Zare, A. Hasaninejad, RSC Adv. 2 (2012) 8010.
[15] A. Zare, F. Abi, A.R. Moosavi-Zare, M.H. Beyzavi, M.A. Zolfigol, J. Mol. Liq. 178 (2013) 113.
[16] M.A. Zolfigol, A. Khazaei, A.R. Moosavi-Zare, A. Zare, Z. Asgari, V. Khakyzadeh, A. Hasaninejad, Ind. Eng. Chem. Res. 19 (2013) 721.
[17] M. Karami, A. Zare, Z. Naturforsch. B 73 (2018) 289.
[18] A.R. Moosavi-Zare, M.A. Zolfigol, E. Noroozizadeh, V. Khakyzadeh, A. Zare, M. Tavasoli, Phosphorus Sulfur Silicon Relat. Elem. 189 (2014) 149.
[19] A.R. Moosavi-Zare, M.A. Zolfigol, E. Noroozizadeh, M. Tavasoli, V. Khakyzadeh, A. Zare, New J. Chem. 37 (2013) 4089.
[20] M. Zolfigol, V. Khakyzadeh, A. Moosavi-Zare, G. Chehardoli, F. Derakhshan-Panah, A. Zare, O. Khaledian, Sci. Iran. 19 (2012) 1584.
[21] S. Babaee, M.A. Zolfigol, M. Zarei, J. Zamanian, ChemistrySelect 3 (2018) 8947.
[22] M.S. Saini, A. Kumar, J. Dwivedi, R. Singh, Int. J. Pharm. Sci. Res. 4 (2013) 66.
[23] K. Ajay Kumar, N. Renuka, G. Vasanth Kumar, D. Lokeshwari, J. Chem. Pharm. Res. 7 (2015) 693.
[24] A.E.-F.G. Hammam, 37 (2005) doi =https://doi.org/10.1002/chin.200602131.
[25] M. Benchekroun, L. Ismaili, M. Pudlo, V. Luzet, T. Gharbi, B. Refouvelet, J. Marco-Contelles, Future Med. Chem. 7 (2015) 15.
[26] R.K. Razdan, R.J. Bruni, A.C. Mehta, K.K. Weinhardt, Z.B. Papanastassiou, J. Med. Chem. 21 (1978) 643.
[27] H. Nakajima, B. Sato, T. Fujita, S. Takase, H. Terano, M. Okuhara, J. Antibiot. 49 (1996) 1196.
[28] B. Cerdá, J.C. Espín, S. Parra, P. Martínez, F.A. Tomás-Barberán, Eur. J. Nutr. 43 (2004) 205.
[29] T.K. Chattapadhyay, P. Dureja, J. Agric, Food Chem . 54 (2006) 2129.
[30] A.H. Bedair, H.A. Emam, N.A. El-Hady, K.A. Ahmed, A.M. El-Agrody, Il Farmaco 56 (2001) 965.
[31] B. Maleki, M. Baghayeri, S. Sheikh, S. Babaee, S. Farhadi, Russ. J. Gen. Chem. 87 (2017) 1064.
[32] M.G. Dekamin, M. Eslami, A. Maleki, Tetrahedron 69 (2013) 1074.
[33] H.R. Shaterian, M. Mohammadnia, J. Mol. Liq. 177 (2013) 353.
[34] S.M. Baghbanian, RSC Adv. 4 (2014) 59397.
[35] S.H. Banitaba, J. Safari, S.D. Khalili, Ultrason. Sonochem. 20 (2013) 401.
[36] R.M.N. Kalla, M.R. Kim, I. Kim, Tetrahedron Lett. 56 (2015) 717.
[37] M. Zarei, Iran. J. Catal. Spotlight (2019) in press.
[38] M. Zarei, Iran. J. Catal. Spotlight 8 (2018) 237.
[39] A.R. Moosavi-Zare, M.A. Zolfigol, M. Zarei, A. Zare, V. Khakyzadeh, A. Hasaninejad, Appl. Catal. A Gen. 467 (2013) 61.
[40] N.M. Logacheva, V.E. Baulin, A.Y. Tsivadze, E.N. Pyatova, I.S. Ivanova, Y.A. Velikodny, V.V. Chernyshev, Dalton Trans. (2009) 2482.
[41] H. Bonadeo, E. Silberman, J. Mol. Spectrosc. 32 (1969) 214.
[42] J.M. Khurana, B. Nand, P. Saluja, Tetrahedron 66 (2010) 5637.
[43] B. Maleki, Org. Prep. Proced. Int. 48 (2016) 81.
[44] M.A. Ghasemzadeh, Z. Elyasi, M. Azimi-Nasrabad, B. Mirhosseini-Eshkevari, Comb. Chem. High Throughput Screen. 20 (2017) 64.
[45] A. Upadhyay, V.K. Singh, R. Dubey, N. Kumar, L. Sharma, R.K.P. Singh, Tetrahedron Lett. 58 (2017) 4323.
[46] M.N. Khan, S. Pal, S. Karamthulla, L.H. Choudhury, RSC Adv. 4 (2014) 3732.
[47] R. Teimuri-Mofrad, S. Esmati, M. Rabiei, M. Gholamhosseini-Nazari, J. Chem. Res. 42 (2018) 7.
[48] B. Sadeghi, P.F. Nezhad, S. Hashemian, J. Chem. Res. 38 (2014) 54.
[49] F. Abdelrazek, M. Helal, A. Hebishy, S. Hassan, J. Heterocycl. Chem. 52 (2015) 1026.
[50] H. Knözinger, S. Huber, J. Chem. Soc. Faraday Trans. 94 (1998) 2047.
[51] M. Quinteiro, C. Seoane, J. Soto, Revue Roumaine DE Chimie 24 (1979) 859.
[52] X.H. Wang, X.H. Zhang, S.J. Tu, F. Shi, X. Zou, S. Yan, Z.G. Han, W.J. Hao, X.D. Cao, S.S. Wu, J. Heterocycl. Chem. 46 (2009) 832.
[53] J. Safaei-Ghomi, F. Eshteghal, H. Shahbazi-Alavi, Ultrason. Sonochem. 33 (2016) 99.
[54] M. Kangani, N. Hazeri, A. Yazdani-Elah-Abadi, M.T. Maghsoodlou, J. Chin. Chem. Soc. 64 (2017) 1259.